A Multi-Dimensional Approach to Carbodiphosphorane-Bismuth Coordination Chemistry: Cationization, Redox-Flexibility, and Stabilization of a Crystalline Bismuth Hydridoborate

Akachukwu D. Obi,[1] Diane A. Dickie,[1] William Tiznado,[2] Gernot Frenking,[3] Sudip Pan,[3] and Robert J. Gilliard, Jr.[1*]*

[1]Department of Chemistry, University of Virginia, 409 McCormick Road, PO Box 400319, Charlottesville, Virginia 22904, United States

[2]Computational and Theoretical Chemistry Group, Departamento de Ciencias Químicas, Facultad de Ciencias Exactas, Universidad Andres Bello, República 498, Santiago, Chile.

[3]Philipps-Universität Marburg Hans-Meerwein-Straße, 35032 Marburg, Germany.

ABSTRACT. Bismuth complexes stabilized by carbon-based donor ligands are underserved by their instability often due to facile ligand dissociation and deleterious protonolysis. Herein, we show that the *ortho*-bismuthination of hexaphenylcarbodiphosphorane (CDP) enables a robust framework with geometrically-constrained carbone-bismuth bonding interactions, which are highly tunable by cationization. The carbodiphosphoranyl bismuth halides (**1** and **2**) are remarkably air-stable, and feature unprecedented *trans* ^{carbone}C–Bi–X ligation, resulting in highly elongated Bi–X bonds. In contrast to known carbone-bismuth complexes, hydrolytic activation of the carbone yields well-defined organobismuth complexes, and subsequent dehydrohalogenation is feasible using potassium bis(trimethylsilyl)amide or N-heterocyclic carbenes. The redox-flexibility of this framework was evaluated in the high catalytic activity of **1** and **2** for silylation of 2,2,6,6-tetramethylpiperidin-1-oxyl (TEMPO) under mild conditions (50 ºC, 24 – 96 h) and low catalyst loadings (5 – 10 mol%), which suggests the accessibility of short-lived hydridic and radical bismuth species. The reaction of **1**, $PhSiH_3$ and tris(pentafluorophenyl)borane (BCF) yield the first crystallographically characterized bismuth hydridoborate complex as an ionic species (**9**), presumably by BCF-mediated hydride abstraction from an unobserved [Bi]–H intermediate. All isolated compounds have been characterized by heteronuclear NMR spectroscopy and X-ray crystallography, and the bonding situation in representative complexes (**1**, **2**, **5** and **9**) were further evaluated using density functional theory (DFT).

INTRODUCTION

In recent years, the organometallic chemistry of bismuth has re-emerged as a hot topic across multiple areas of synthetic chemistry and catalysis.[1-5] Bismuth is particularly appealing due to its non-toxic and environmentally benign nature, which may have future implications in the development of chemical transformations that do not rely on toxic or precious metals.[6] Owing to high-lying, partially-filled orbitals, low-valent bismuth compounds are well-positioned to mimic the synergistic effect of *d*-orbitals in challenging bond activation events.[7-10] Despite these positive attributes, isolating well-defined bismuth complexes can be synthetically challenging due to the ease at which many compounds undergo thermal decomposition to bismuth metal or the corresponding oxy-salts. Indeed, the poor spatial overlap of atomic orbitals in bismuth compounds results in metastable Bi–X bonds (X = Bi, O, C, N, P, S, etc.) with low homolytic dissociation energies.[6] However, this property can be harnessed by rational ligand stabilization strategies[11-13] towards productive bond activations and radical redox transformations.[1, 14-22] To this end, electronically-flexible pincer ligands are desirable for their tunable stereoelectronics due to redox-flexible pendant arms with bulky groups for kinetic stabilization, and/or weakly coordinating backbone heteroatoms for tuning their reactivities (Figure 1).[2, 11, 23] This strategy enabled the elucidation of monomeric Bi(II) radicals (e.g., **I-III**, Figure 1a) as transient or isolable intermediates in stoichiometric and catalytic transformations.[14-19, 24-26] Notably, Chitnis exploited the redox noninnocence of a triamide ligand towards a "redox-confused" Bi(I/III) complex (**IV**, Figure 1b) with

electromorphic reactivity, for example in its Lewis acidity towards pyridine oxide or basicity towards $W(CO)_5$.[27] Bi(I)/Bi(III) transformations are especially difficult,[28] and the first implementation of such a redox cycle in catalysis was achieved by Cornella,[29] enabled by an *NCN*-bismuthinidene introduced by Dostál (**V**, Figure 1c).[30] Although Bi(III) and Bi(V) complexes are significantly more stable than their low valent counterparts, Bi(III)/Bi(V) redox catalysis is similarly an emerging phenomenon, only recently established by a tethered ligand framework with auxiliary weakly-coordinating sulfone (**VI**).[20]

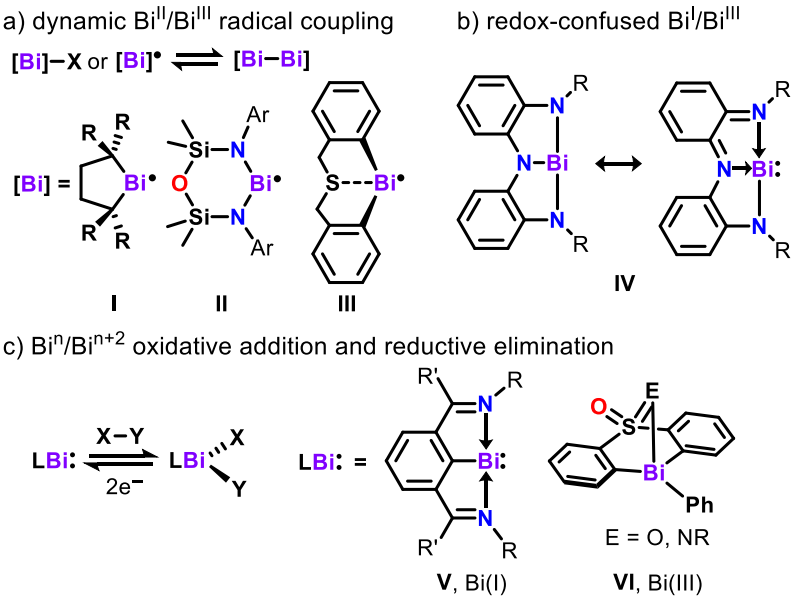

Figure 1. Selected examples of redox-flexible bismuth platforms highlighting design strategies based on pincer ligands and/or redox-flexible electronegative elements (R = alkyl, silyl, aryl).

Our interest concerns the paucity of bismuth-mediated transformations involving electronically-flexible, carbon-based donor ligands (i.e., carbenes and carbones). Despite the versatility of these ligands in light *p*-block element chemistry,[31] relevant studies concerning

the heavier elements are comparatively rare.[32] Coordination adducts of Bi(III) complexes and N-heterocyclic carbenes (NHCs) and cyclic(alkyl)(amino) carbenes (CAACs) are highly sensitive to small changes in their coordination environment, and prone to rapid decomposition in solution.[33-39] For example, Bi(III) complexes of N-heterocyclic carbenes (NHC) bearing an unsaturated backbone (i.e., 1,3-bis(2,6-diisopropylphenyl)-imidazol-2-ylidene or IPr) are subject to thermal isomerization to abnormally bonded mesoionic complexes, while those involving the saturated NHC 1,3-bis(2,6-diisopropylphenyl)-4,5-dihydroimidazole-2-ylidene (SIPr) require THF-solvation for stabilization, without which they rapidly decompose to intractable mixtures.[34, 35] Notably, the π-acidity of CAACs enabled the isolation and crystallographic elucidation of two-coordinate bismuthinidenes [(CAAC)Bi(Ph)][38] and [(CAAC)$_2$Bi][OTf],[39] involving partial C←:Bi π-backbonding interactions. These complexes are also highly reactive and rapidly decompose under ambient conditions. Contrarily, carbones such as carbodiphosphoranes (CDPs)[40-42] and carbodicarbenes (CDCs)[43-46] are four-electron σ, π-donors, and thus feature stronger ^{carbone}C⇉Bi multiple bonding interactions at Bi(III) centers (Figure 2a).[47] The donor strength of carbones permits isolation of stable low-coordinate monomeric Bi(III) complexes,[47-51] whereas their carbene analogues mostly exist as dimeric complexes in coordinatively saturated octahedral geometries.[33-36] Notwithstanding their enhanced thermal stability, reported carbone-bismuth complexes are similarly disadvantaged by deleterious protonation,[51] and to the best of our

knowledge, there are still no examples of productive bond activation events at bismuth centers stabilized by carbon donor ligands.[3, 32]

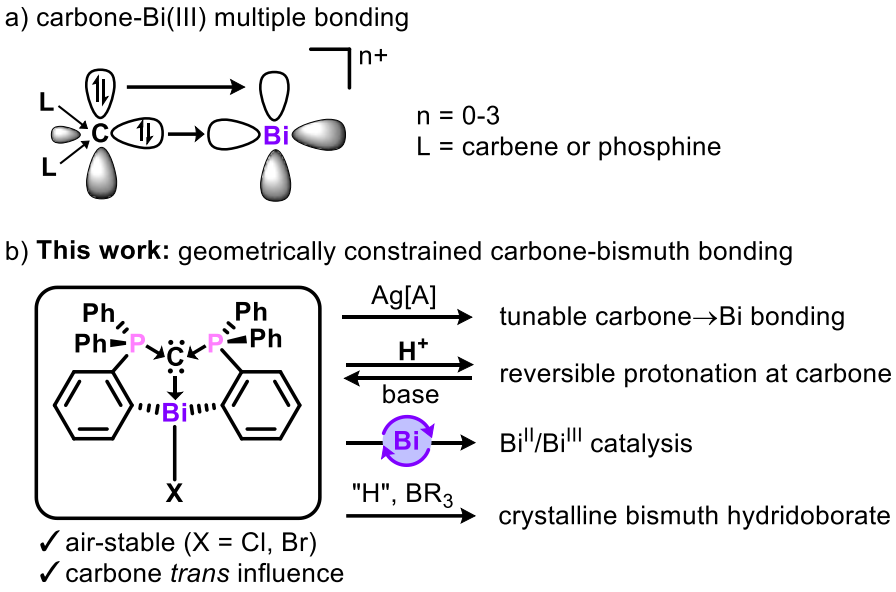

Figure 2. Electronic flexibility in carbone bismuth bonding highlighting (a) non-reductive carbone-Bi(III) multiple bonding via double dative interactions, and (b) a tethered carbodiphosphoranyl bismuth framework with persistent and tunable carbone coordination.

The recent dilithiation of hexaphenylcarbodiphosphorane[41] by Sundermeyer afforded a dianionic, *CCC*-pincer ligand [Li_2(CDP)],[52] which retains a four-electron σ,π-donor central carbone, and can be transferred to organometallic systems by simple halide metathesis reactions.[53] Inspired by the coordinative flexibility of this ligand, we were motivated to investigate its ability to stabilize redox-flexible bismuth reagents as part of our ongoing investigations into the electronic influence of carbones at heavy pnictogen complexes.[47] We now report the isolation and reactivities of air-stable carbodiphosphoranyl (CDP)[54]

bismuth(III) halides (**1** and **2**), which can be easily ionized with highly tunable ^{carbone}C–Bi bonding in the monocations **3-10**. Their electronic configuration is comparable to pnictogen complexes of methanide $[R_3C:]^-$ and methanediide $[R_3C::]^{2-}$ ligands with auxiliary stabilization from pendant heteroatoms (e.g., *NCN*[48, 50] or *SCS*[49] vs *CCC* in this work). However, the exclusion of chelating heteroatoms herein discourages protonolysis of the pendant arms by carbone-heteroatom proton shuttling (e.g., ^{ylide}CH↔^{imine}NH tautomerism),[48] and thus enables robust ligand coordination (Figure 2b). Thus, protolytic activation of the carbone center is reversible and maintains metal-ligand coordination, in contrast to the case for neutral carbone ligands whereby ligand protonation results in destabilized species.[51] Having established its robust coordination, we investigated the capacity of this framework for low valent redox transformations in the rapid catalytic silylation of 2,2,6,6-tetramethylpiperidin-1-oxyl (TEMPO), whereby **1** and **2** demonstrated higher or competitive activity compared to known Bi(II) platforms.[15, 16, 26] Preliminary mechanistic studies led to isolation of the first crystallographically characterized bismuth hydridoborate (**9**).

RESULTS AND DISCUSSION

Carbone *Trans* Influence in the Isolation of Carbodiphosphoranyl Bismuth(III) Halides. The reaction of equimolar amounts of Li_2(CDP) and $BiCl_3$ or $BiBr_3$ afforded the organobismuth(III) halides (CDP)BiCl (**1**) and (CDP)BiBr (**2**) respectively, in 70-80% yields (Scheme 1). In contrast to the vibrant colors of monodentate CDP bismuth(III) halides,[51] compounds **1** and **2** are colorless solids. There is also little differentiation in the spectroscopic signatures of **1** and **2**.

The CDP phosphorus resonance in **1** (δ_P 38.4 ppm) and the highly deshielded *ortho* C*H*–CBi doublet (δ_H 9.32 ppm) compare with the same for **2** (δ 38.6 ppm and 9.34 ppm respectively). In the $^{13}C\{^1H\}$ NMR spectra, the ylidic carbon resonances for **1** (δ_C 24.0 ppm, $^1J_{PC}$ = 98 Hz) and **2** (δ_C 23.3 ppm, $^1J_{PC}$ = 98 Hz) are significantly upfield from the monodentate (CDP)$BiCl_3$ adduct (δ_C 66.8 ppm, $^1J_{PC}$ = 72 Hz),[51] due to the electron donating phenyl groups in their coordination sphere.

Scheme 1. Stabilization of bismuth halides at a dianionic carbodiphosphoranyl framework

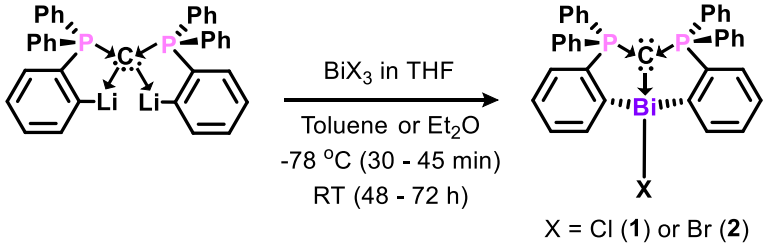

Colorless, block-like single crystals of **1** and **2** were obtained from their respective saturated DCM/hexanes solutions at room temperature.[55] Single crystal X-ray diffraction (SC-XRD) analysis revealed mononuclear structures, wherein the bismuth atom lies within a distorted see-saw geometry comprised of one tridentate CDP ligand and one halide atom (Figure 3). The metrical parameters for the CDP ligand in **1** and **2** are nearly identical within standard deviation (Figure 3 caption), with the exception of a slightly wider ligand bite angle in **2** (C3–Bi1–C21 is 98.32(16)º in **1** and 102.12(11)° in **2**). There are substantial intramolecular π-interactions between the *cis* "backbone" phenyl substituents [P1(Ph)---(Ph)P2 centroid distances: 3.646(3) Å (**1**) and 3.791(2) Å (**2**)], which may impose further rigidity on the ligand framework. However, the most remarkable feature in their molecular structures is an

unprecedented *trans* carbone influence for pnictogen complexes, whereby the donor carbone atom is *trans* to a functional group (^{carbone}C–Bi–halide is 163.30(12)° in **1** and 165.31(8)° in **2**). The pronounced carbone donor strength imbues much greater *trans* influence than known *trans* donor–Bi–X examples,[56-60] resulting in highly elongated Bi–halide bonds in **1** [3.0110(11) Å] and **2** [3.0826(4) Å]. Indeed, there is only a small difference between the Bi–Cl and Bi–Br bond lengths (Δ 0.072 Å), which are themselves more closely correlated with contacts between Bi and weakly-coordinated anions or halogenated solvents than those of typical covalent Bi–Cl ($\sum R_{cov}$ = 2.50) and Bi–Br ($\sum R_{cov}$ = 2.65) bonds.[61]

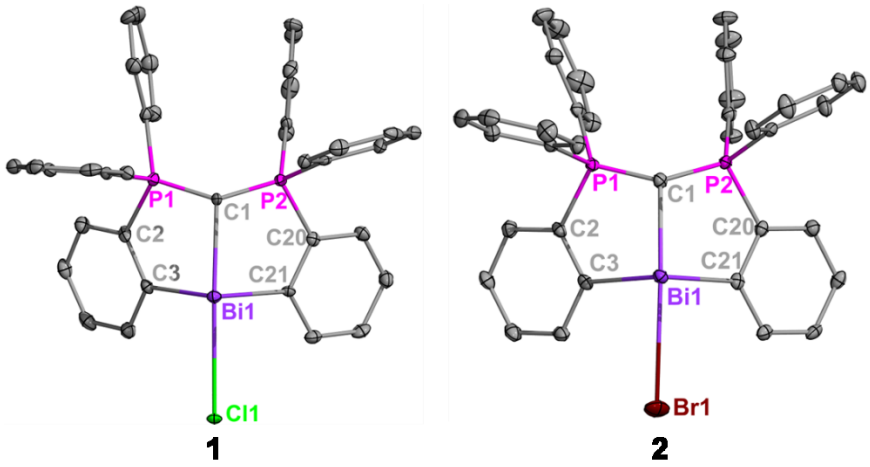

Figure 3. Molecular structures of **1** and **2**. Thermal ellipsoids set at 50% probability. Co-crystallized dichloromethane molecules and all H atoms are omitted for clarity. Selected bond distances (Å) and angles (°) for **1** [and **2**]: Bi1–C1, 2.368(4) [2.346(3)]; Bi1–Cl1, 3.0110(11) [Bi1–Br1, 3.0826(4)]; Bi1–C3, 2.279(4) [2.273(3)]; Bi1–C21, 2.268(4) [2.275(3)]; C1–P1, 1.677(4)

[1.680(3)]; C1–P2, 1.692(4) [1.686(3)]; C1–Bi1–Cl1, 163.30(12) [C1–Bi1–Br1, 165.31(8)]; C3–Bi1–C21, 98.32(16) [102.12(11)]; P1–C1–P2, 132.2(3) [134.9(2)].

Compounds **1** and **2** are highly soluble in dichloromethane (DCM) and chloroform, and indefinitely stable under anaerobic and anhydrous conditions in both solid- and solution-states. In contrast to the highly air- and moisture-sensitive monodentate carbone-bismuth(III) halides, **1** and **2** are bench-top-stable under air for at least one week. Furthermore, no degradation was spectroscopically observed when **1** and **2** were monitored for two months in hydrated CD_2Cl_2, containing a stoichiometric amount of water. However, the addition of excess water to these solutions resulted in the precipitation of sticky solids presumed to be metal hydroxides.

Stabilization of Low-Coordinate Ionic Bismuth(III) Complexes

In an effort to isolate reactive, low coordinate complexes, we investigated the cationization of **1** and **2** using halide abstraction reagents. The reaction of **1** and $Ag[NTf_2]$ in THF or DCM resulted in incomplete halide abstraction to form the ionic complex $[((CDP)Bi)_2(\mu\text{-}Cl)][NTf_2]$ (**3[NTf$_2$]**, Scheme 2). Notably, **3[NTf$_2$]** may be considered a coordination adduct of **1** and the targeted ionic complex $[(CDP)Bi][NTf_2]$, which could not be isolated despite prolonged reaction times. The isostructural adducts **3[BPh$_4$]** and $[((CDP)Bi)_2(\mu\text{-}Br)][BPh_4]$ (**4[BPh$_4$]**) were isolated from reactions of $NaBPh_4$ with **1** and **2** respectively, but additional reaction times (16 - 48 h) enabled complete halide abstraction to obtain $[(CDP)Bi][BPh_4]$ (**5[BPh$_4$]**) in high yields (> 94%). The likewise reaction of **1** and $Na[BAr^{F}{}_4]$

(Ar^F = 3,5-$(CF_3)_2C_6H_3$) afforded **5[BAr^F_4]**, which exhibits improved solubility in common organic solvents (Et_2O, THF, CH_2Cl_2) in contrast to **5[BPh_4]** which is highly soluble in DCM but poorly soluble in ethers. The utilization of fluoride-rich silver salts for cationization afforded **5[BF_4]** and **5[SbF_6]** in much shorter reaction times (30 min, Scheme 2). The $^{31}P\{^1H\}$ resonances of **3**-**5** are downfield from those of **1** and **2**, and their chemical shifts increased with sequential halide abstraction (Table 1), which suggests electron deficiency at the phosphorus atoms due to increased carbone–bismuth interactions.

Scheme 2. Cationization of **1** and **2** towards stronger ^{carbone}C–Bi bonding

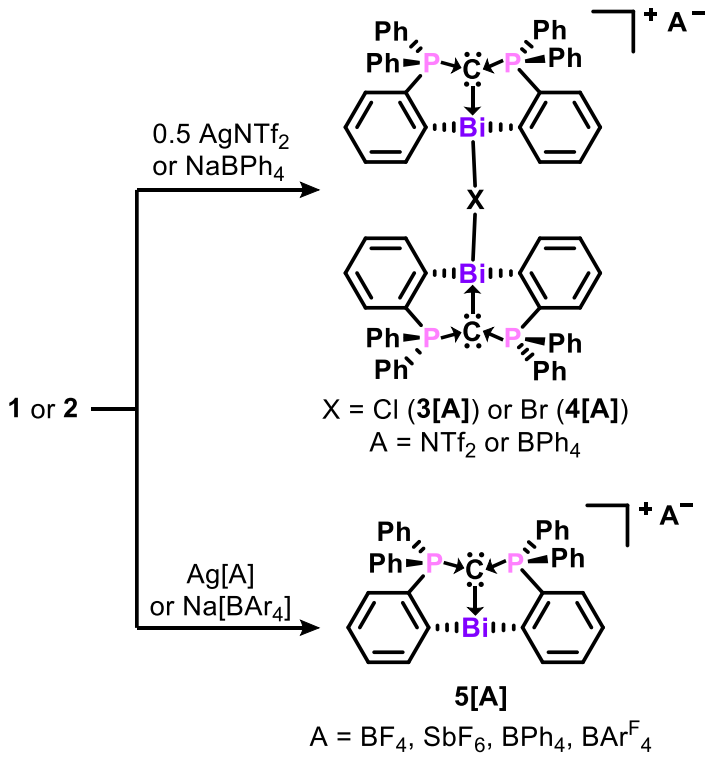

X-ray quality single crystals of **3**-**5** were obtained from their respective layered DCM/hexanes solutions at room temperature, and their molecular structures are described in

Figure 4. Compounds **3[NTf$_2$]**, **3[BPh$_4$]** and **4[BPh$_4$]** are dimeric molecules with isostructural cationic units wherein the CDP-stabilized bismuth centers are symmetrically bridged by a single halide, and balanced by a non-coordinating anion (Figure 4 and Figure S16). Their ^{carbone}C–Bi bonds are expectedly shortened from **1** and **2**, but their halide contacts are comparable, which further highlights the labile or weakly-coordinating nature of the halides. Notably, the Bi–X–Bi bond angles of 166.55°, 172.75(8)° and 167.49(6)° in **3[NTf$_2$]**, **3[BPh$_4$]** and **4[BPh$_4$]** respectively are on the wider end of reported values for (LBi)$_2$(μ-X) complexes (152 – 172°).[25, 57] The molecular structures of **5[BF$_4$]** and **5[SbF$_6$]** each feature one Bi---F contact from the anion, which is shorter in **5[BF$_4$]** (2.891(3) Å) than **5[SbF$_6$]** (2.926(6) Å). In **5[BPh$_4$]**, a close Bi---Ph(BPh$_3$) centroid distance (3.870 Å) indicates non-negligible cation-anion interactions, but similar interactions were not observed in **5[BAr$^F_4$]** likely owing to the π-electron deficient nature of the Ar^F groups, and the bismuth center is truly tricoordinate. Although the atom connectivity in **5[BAr$^F_4$]** is unambiguous, confident analysis of its bond metrices is hindered by poor crystal data due to weak diffraction.

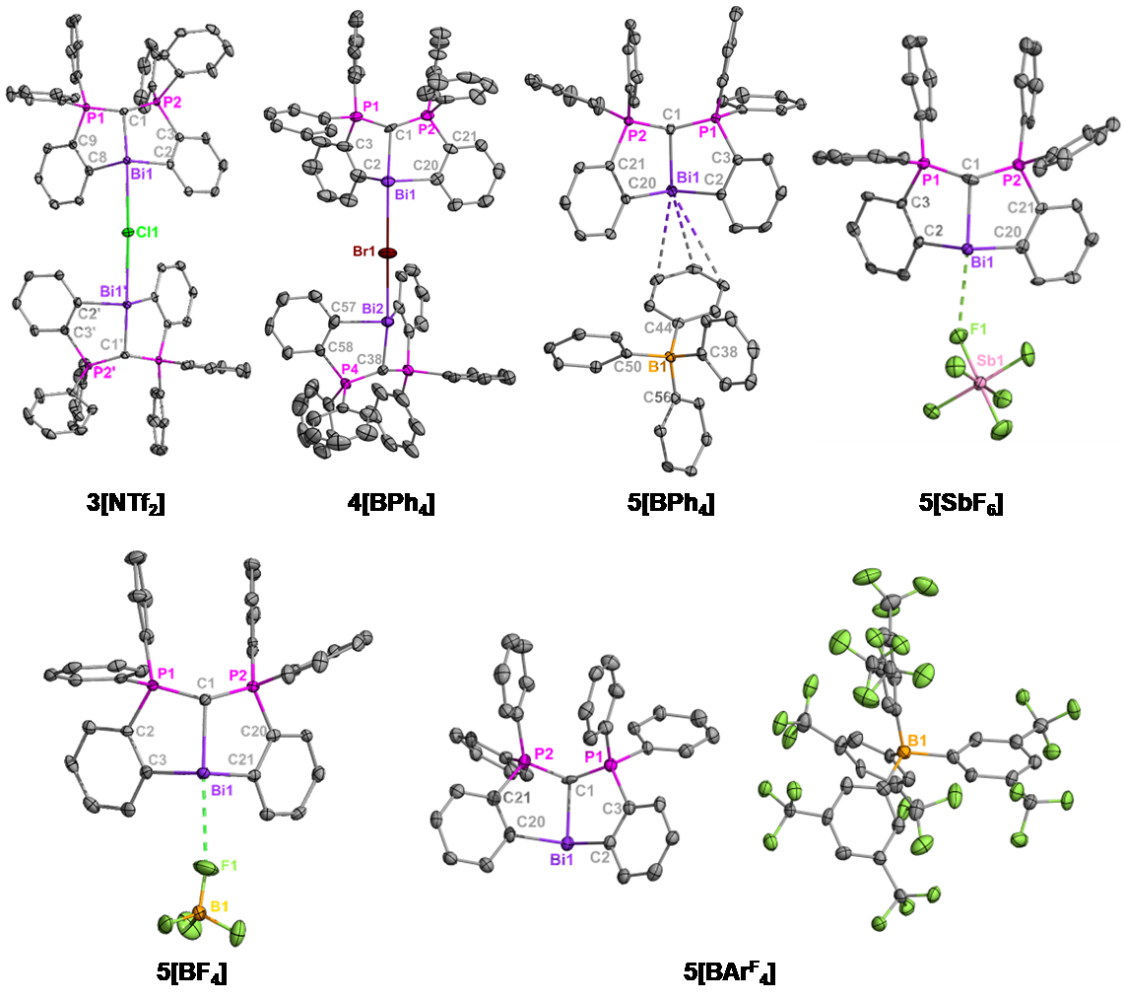

Figure 4. Molecular structures of **3**-**5**. A non-coordinating bis(triflimide) anion in **3[NTf2]**, tetraphenylborate anion in **4[BPh4]**, co-crystallized solvent molecules, and all H atoms are omitted for clarity. Selected bond distances (Å) and angles (°): **3[NTf2]**: Bi1–C1, 2.295(2); Bi1–Cl1, 3.0939(3); Bi1–C2, 2.258(2); Bi1–C8, 2.290(2); C1–P1, 1.684(2); C1–P2, 1.691(2); C2–Bi1–C8, 100.46(8); P1–C1–P2, 128.7(14). **4[BPh4]**: Bi1–C1, 2.291(11); Bi1–Br1, 3.0947(15); Bi2–Br1, 3.1184(15); Bi1–C2, 2.286(11); Bi1–C20, 2.258(11); C1–P1, 1.691(12); C1–P2, 1.674(11); C2–Bi1–C8, 101.7(4); P1–C1–P2, 131.5(8). **5[BF4]**: Bi1–C1, 2.275(4); Bi1---F1, 2.891(3); Bi1–C3, 2.260(5); Bi1–C21, 2.253(5); C1–P1, 1.704(5); C1–P2, 1.699(5); C3–Bi1–C21, 93.96(17); P1–C1–

P2, 130.1(3). **5[SbF$_6$]**: Bi1–C1, 2.269(8); Bi1---F1, 2.926(6); Bi1–C2, 2.272(8); Bi1–C20, 2.257(8); C1–P1, 1.673(10); C1–P2, 1.712(9); C2–Bi1–C20, 96.4(3); P1–C1–P2, 131.3(5). **5[BPh$_4$]**: Bi1–C1, 2.275(3); Bi1–C2, 2.261(3); Bi1–C20, 2.252(3); C1–P1, 1.692(3); C1–P2, 1.698(3); C2–Bi1–C20, 96.95(10); P1–C1–P2, 132.33(18). **5[BAr$^F_4$]**: Bi1–C1, 2.219(10); Bi1–C2, 2.227(14); Bi1–C20, 2.290(13); C1–P1, 1.705(16); C1–P2, 1.684(15); C2–Bi1–C20, 102.3(6); P1–C1–P2, 132.6(7).

Table 1. Selected Spectroscopic for **1-6**

	δ ^{31}P (ppm)	δ ^{13}C (ppm)[a]	$^1J_{PC}$ (Hz)[a]
1	38.4	24.0	98
2	38.6	23.3	98
3[NTf$_2$]	43.9	22.1	96
3[BPh$_4$]	47.0	20.8	94
4[BPh$_4$]	45.5	21.2	96
5[BF$_4$]	48.9	-	-
5[SbF$_6$]	51.5	18.8	92
5[BPh$_4$]	50.4	19.2	93
5[BAr$^F_4$]	53.3	18.7	93
6[BPh$_4$]	28.1	18.6	71

[a]Ylidic carbon.

Compounds **3-5** are extremely moisture sensitive, yielding structurally similar ionic complexes of the type [(H-CDP)BiX][A] (**6**-**8**; X, A = halide and/or weakly coordinating anion) due to protonolysis of adventitious moisture in the reaction solvents (Figure 5). Remarkably,

6-**8** are metalated complexes with tridentate CDP coordination to bismuth, which contrasts deleterious metal-ligand dissociation in the protonation of monodentate carbone-bismuth complexes.[47, 51] In their molecular structures, an elongation of the ^{carbone}C–P bonds towards single bond regimes suggests elimination of the characteristic carbodiphosphorane C–P multiple bonds, and further reflects in the tetrahedral arrangement of the C1 carbon. Consequently, their P1–C1–P2 bond angles (range 120.4(3)° – 124.2(3)°) are contracted from those of **1**-**5** (128.7° – 134.9°). The Bi–halide bonds in **6** and **7** are comparable to typical terminal bismuth(III)-halide contacts in the literature, and significantly shortened from those of **1** and **2**, as the *trans*-influence of the carbone is eliminated by protonation (see Figure 5 caption).

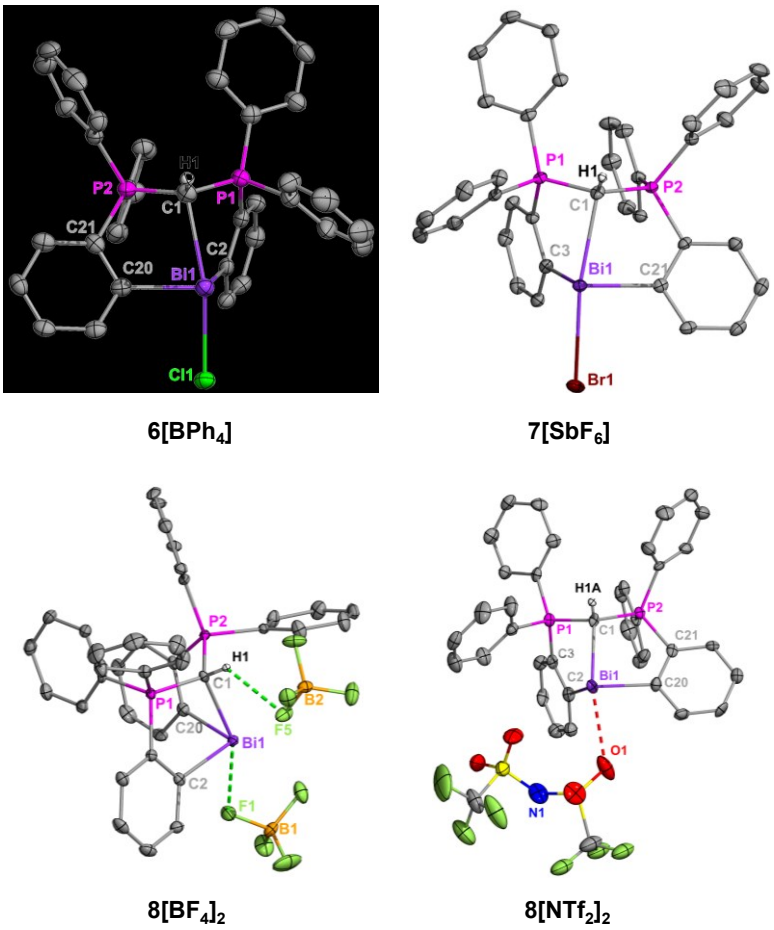

Figure 5. Molecular structures of **6-8**. Thermal ellipsoids shown at 50 % probability. Non-coordinating anions (for **6**[BPh_4], **7**[SbF_6] and **8**[NTf_2]$_2$) and aromatic protons are omitted for clarity. Only the major occupied position for disordered atoms in **8**[NTf_2]$_2$ is shown. Selected bond distances (Å) and angles (°): **6**[BPh_4]: Bi1–C1, 2.609(5); Bi1–Cl1, 2.6324(14); Bi1–C2, 2.281(5); Bi1–C20, 2.263(5); C1–P1, 1.739(5); C1–P2, 1.763(6); C2–Bi1–C20, 102.97(18); P1–C1–P2, 124.2(3). **7**[SbF_6]: Bi1–C1, 2.615(3); Bi1–Br1, 2.8461(4); Bi1–C3, 2.297(3); Bi1–C21, 2.281(3); C1–P1, 1.750(3); C1–P2, 1.765(3); C3–Bi1–C21, 100.22(9); P1–C1–P2, 122.07(16). **8**[BF_4]$_2$: Bi1–C1, 2.416(6); Bi1–F1, 2.657(3); Bi1–C2, 2.251(4); Bi1–C20, 2.285(5); C1–P1,

1.795(6); C1–P2, 1.781(4); C2–Bi1–C20, 95.45(15); P1–C1–P2, 120.4(3). **8[NTf$_2$]$_2$**: Bi1–C1, 2.411(6); Bi1···O1, 2.841(7); Bi1–C2, 2.290(6); Bi1–C20, 2.244(7); C1–P1, 1.780(6); C1–P2, 1.793(7); C2–Bi1–C20, 98.3(2); P1–C1–P2, 120.6(3).

Although **6-8** were typically isolated in trace amounts as decomposition products, the intentional protonation of **1** using Evans' reagent [HNEt$_3$][BPh$_4$][62] afforded [(H-CDP)BiCl][BPh$_4$] (**6[BPh$_4$]**) in 84% yield, and permitted further spectroscopic analyses (Scheme 3). A prominent triplet resonance due to the C1 proton (δ_H 2.74 ppm, $^2J_{PH}$ 6.5 Hz) is observed in the ^{1}H NMR spectrum of **6[BPh$_4$]**, and the phosphorus resonance (δ_P 28.1 ppm) is significantly upfield from those of **1**-**5** (see Table 1). In the ^{13}C{^{1}H} NMR spectrum, the central carbon (δ_C 18.6 ppm, $^1J_{PC}$ 71 Hz) extends a much smaller coupling constant with the neighboring phosphorus atoms than those of **1**-**5**, which suggests further deviation from carbone character and C–P multiple bonding. Notably, **6[BPh$_4$]** may be selectively and quantitatively deprotonated by dehydrohalogenation to **1** or **5[BPh$_4$]** using an unencumbered *N*-heterocyclic carbene (NHC = 1,3-diisopropyl-4,5-dimethylimidazol-2-ylidene) or potassium bis(trimethylsilyl)amide respectively (Scheme 3).

Scheme 3. Formation and dehydrohalogenation of **6[BPh$_4$]**

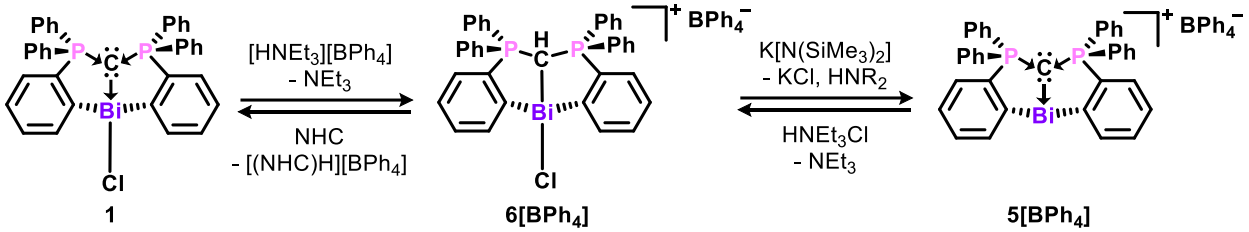

Notably, the bonding configuration in **6-8** is comparable to bis(iminophosphorane) methanide (BIPM) pnictogen complexes,[48, 50] although the introduction of BIPM at bismuth resulted in intractable mixtures due in part to ^{ylide}C–H ↔ ^{imine}N–H tautomerization.[48] Thus, the exclusion of chelating heteroatoms in this CDP framework discourages protonolysis of the pendant arms by carbone-heteroatom proton shuttling and enables robust ligand coordination.

Involvement of Carbodiphosphoranyl Bismuth Halides in Redox Catalysis and Isolation of a Bismuth Hydridoborate Complex

Having realized that the ionization of **1** and **2** involves facile tuning of ^{carbone}C–Bi interactions, we probed the impact of this donor interaction in redox transformations at bismuth. The reaction of **1** or **2** and stoichiometric equivalents of alkali-metal-based reducing agents (e.g., KC_8, Na, K[$HBEt_3$] and Li[$HBEt_3$]) resulted in slow decomposition (over 3 h) to an intractable mixture of products. We suspect that these reductions result in the formation of an unstable bismuth radical, as a combination of unfavorable sterics and carbone *trans* effect may hinder the stabilization of a Bi–Bi bond within this framework. The utilization of milder reducing agents (e.g., $PhSiH_3$, [Mg^I][63]) yielded no reaction with **1** under ambient conditions, although the addition of excess $PhSiH_3$ (> 10 equiv.) resulted in partial decomposition with deposition of black solids presumed to be metallic bismuth. Spectroscopic analyses of the latter reaction indicate that **1** persists in solution even after one week, likely owing to a dynamic process between **1** and [Bi]–H (which is unobserved). Consequently, the accessibility of

transient [Bi]–H and $[Bi^{II}]^{\cdot}$ species was probed via the addition of (2,2,6,6-tetramethylpiperidin-1-yl)oxyl (TEMPO).

Isolable $[Bi^{II}–Bi^{II}]$ or $[Bi^{II}]^{\cdot}$ species have been shown to undergo thermal or photochemical Bi–O homolysis in their reactions with TEMPO, which enables catalytic dehydrocoupling of silanes and TEMPO via putative [Bi]–H intermediates.[15, 16, 26] However, thermally activated dehydrocoupling reactions involving bismuth are typically sluggish in comparison to photochemical reactions as highlighted in recent studies by Lichtenberg.[16, 26] Considering the unstable nature of the presumed radical and hydride intermediates within the (CDP)Bi framework, we hypothesized that, if accessible, their catalytic activity under thermal conditions may compete with established systems. Indeed, the addition of excess $PhSiH_3$ to a CD_2Cl_2 solution containing **1** and TEMPO in a 1:10 ratio resulted in a complete disappearance of the red color of TEMPO to yield a colorless solution after 3 d at room temperature (Table 2, entry 1). In contrast to our previous observations, metallic bismuth was not observed until TEMPO was completely consumed in this reaction. Spectroscopic analysis reveals the selective (> 95%) formation of $PhH_2Si(OTEMP)$, as well as the persistence of **1** as the sole phosphorus-containing species.

Table 2. Reactions conditions and conversion data for catalysis experiments

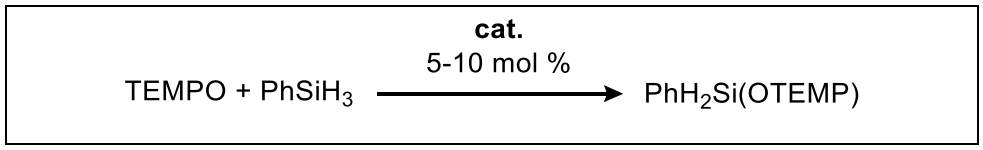

entry	cat. (mol %)	TEMPO/$PhSiH_3$ (equiv)	condition	conversion[a] (%)
control	-	1/1	80 ºC, 48 h	< 1
1	**1** (10)	1/4	25 ºC, 72 h	> 99[b]
2	**1** (8)	1/1	50 ºC, 24 h	> 99[b]
3	**2** (8)	1/1	50 ºC, 16 h	> 99[b]
4	**1** (5)	2/1	50 ºC, 96 h	> 99[b,c]

[a]In all cases, conversion was > 95% selective for $PhH_2Si(OTEMP)$, and entries herein are based on [b]TEMPO consumption or [c]silane consumption.

The reaction of equimolar amounts of TEMPO and $PhSiH_3$ with 8 mol % **1** or **2** required mild heating (50 ºC) for perceptible activity, but the complete consumption of TEMPO and plateaued production of $PhH_2Si(OTEMP)$ was observed after 16 - 24 h (entries 2 and 3). Notably, $PhSiH_3$ was not completely consumed in this reaction, and H_2 was not detected in appreciable quantities in the ^1H NMR spectrum. Although H_2 is not soluble in DCM at the reaction temperatures, an alternate process for hydrogen abstraction towards bismuth radicals is possible. Recent work by Lichtenberg suggests that hydrogen abstraction from the putative [Bi]–H can occur on the glassware surface or via TEMPO to yield TEMPO-H or 2,2,6,6-tetramethylpiperidine (TEMPH) and water.[26] The presence of TEMPO radical in these experiments resulted in broad resonances in the ^1H region where TEMPO-H and TEMPH are expected. Therefore, we performed GC-MS experiments on the reaction solutions and found evidence for 2,2,6,6-tetramethylpiperidine, which was not detected in TEMPO (see

Supporting Information). Indeed, the reaction of a 2:1 ratio of TEMPO and $PhSiH_3$ resulted in the complete consumption of $PhSiH_3$ (entry 4).

Because **1** and **2** are not consumed in these reactions, they are presumed the active (pre)catalysts, and a simplified catalytic cycle inspired by literature[15, 16, 26] has been proposed in Figure S56. Unfortunately, none of the anticipated intermediates ([Bi]–H, $[Bi^{II}]^{\cdot}$, [Bi]–OTEMP) were spectroscopically observed or isolated. We hypothesized that the *trans* influence of the carbone contributes to their instability, which may rationalize their higher activity and selectivity in the thermal dehydrocoupling of TEMPO and $PhSiH_3$ than previously reported bismuth systems.[15, 26] Therefore, we investigated the possible interception of the [Bi]–H intermediate by charge separation for thermodynamic stability. To this end, the Lewis acid tris(pentafluorophenyl)borane [$B(C_6F_5)_3$ or BCF] has found versatile applications in frustrated Lewis pair (FLP) chemistry, and relevant to our investigations, as a hydride abstraction reagent.[64] Indeed, the addition of $B(C_6F_5)_3$ to a mixture of (CDP)BiCl (**1**) and excess $PhSiH_3$ yielded the ionic complex [(CDP)Bi···$HB(C_6F_5)_3$] (**9**) as a light-brown solid (Scheme 4). This reaction proceeds rapidly (15 min) at room temperature with significant deposition of bismuth metal, but can be controlled by reduced temperatures (-35 °C, 1 h) with improved yield (68 %). Upon isolation, **9** is thermally stable and amenable to spectroscopic investigations under ambient conditions.

Scheme 4. Synthesis of a bismuth hydridoborate complex

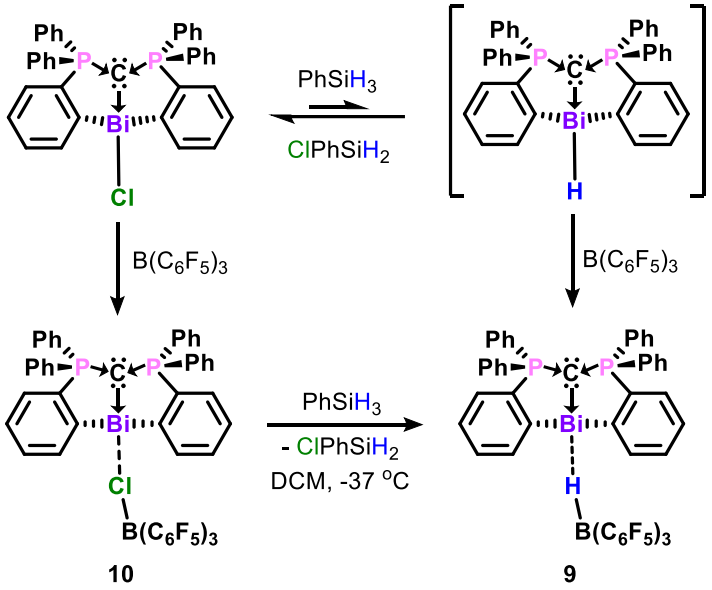

NMR analyses indicate that **9** is a charge-separated species in solution. The CDP phosphorus (δ_P 51.4 ppm) and carbone carbon (δ_C 18.7 ppm, $^1J_{PC}$ 91 Hz) resonances are comparable to those of **5**, and the ^{11}B NMR spectrum reveals a doublet (δ -25.5 ppm, $^1J_{HB}$ 98 Hz) in the expected range for the $\{HB(C_6F_5)_3\}^-$ anion. In the ^{1}H NMR spectrum, the B–H resonance is observed as a 1:1:1:1 quartet at δ 3.60 ppm ($^1J_{BH}$ 96 Hz). The B–H stretch (2310 cm^{-1}) in the solid-state IR spectrum is broadened (Figure S52), suggesting the possibility of secondary interactions with the cation. However, low temperature NMR experiments (up to 203 K) did not yield evidence for Bi---H interactions.

The molecular structure of **9** was confirmed by X-ray diffraction on a single crystal obtained from a layered DCM/hexanes solution, and the anticipated Bi---H contact was unambiguously established in the tripodal coordination of $\{HB(C_6F_5)_3\}^-$ to the metal center (Figure 6a). Due to the high susceptibility of bismuth centers to deleterious reduction, isolable

compounds involving any kind of bismuth-hydride contact are rare,[65] and only one example has been crystallographically characterized as (2,6-$Mes_2C_6H_3)_2BiH$ (Mes = mesityl).[66] The latter is a kinetically-stabilized bismuth hydride molecule with a short Bi–H bond (1.94(2) Å) and strong IR absorption band at 1759 cm^{-1}. Conversely, **9** features a much longer Bi–H interaction (3.14(3) Å) as the hydride is expectedly localized on the boron atom. Gentle heating of **9** (50 °C, 1 h) yielded a colorless solid crystallographically identified as an isomorph (**9′**) whereby the Bi–H contact was labilized and no cation-anion interactions are present (Figure 6b). Instead, **9′** features unusual cation-cation interactions with Bi–π(aryl) interactions between neighboring cations (Figure 6c). In the absence of anion interactions, the ^{carbone}C–Bi bond is shortened from 2.2773(18) Å in **9** to 2.2499(13) Å in **9′**. It is therefore clear that this bismuth hydridoborate complex (**9**) benefits from thermodynamic stabilization due to charge-separation. Notably, attempts to stabilize smaller borohydrides (e.g., BH_4^-, $HBEt_3^-$) at this framework are thus far unsuccessful, and likely requires additional steric protection to attenuate their disproportionation reactions (to $[Bi^0]_n$, H_2 and BR_3).

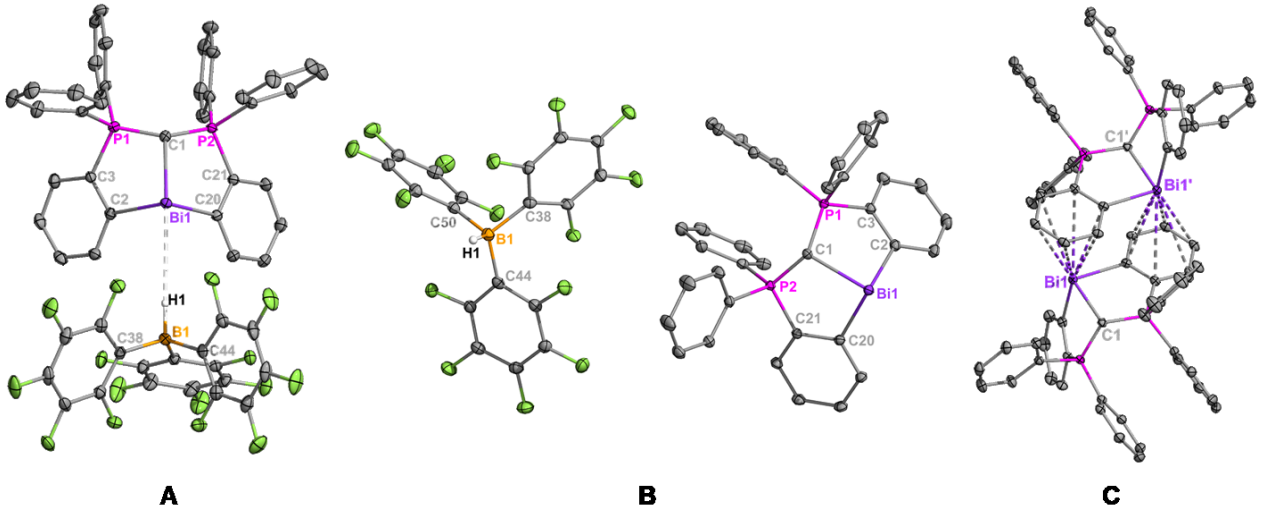

Figure 6. Molecular structures of **9** (A) and **9′** (B), showing cation-cation stacking in **9′** (C). Thermal ellipsoids are shown at 50 % probability, and aromatic protons omitted for clarity. B-H hydrides in **9** and **9′** were isotropically refined. Selected bond distances (Å) and angles (°) for **9** [and **9′**]: Bi1–C1, 2.2773(18) [2.2499(13)]; Bi1–C2, 2.2676(19) [2.2848(14)]; Bi1–C20, 2.2488(18) [2.2498(14)]; Bi1–H1, 3.14(3) [no contact]; C1–P1, 1.6959(19) [1.6993(14)]; C1–P2, 1.6994(19) [1.6998(14)]; C2–Bi1–C20, 95.42(6) [98.11(5)]; P1–C1–P2, 130.10(12) [128.26(8)].

Despite the facile isolation of **9**, a BCF-mediated hydride abstraction from "(CDP)Bi–H" is difficult to substantiate due to the absence of spectroscopic evidence for the bismuth hydride. In the absence of $B(C_6F_5)_3$, the prolonged reaction of **1** and $PhSiH_3$ does not result in complete consumption of **1** (despite evident decomposition to metallic bismuth). Therefore, a dynamic equilibrium which favors the formation of **1** via metathetical reaction of "(CDP)Bi–H" and $ClPhSiH_2$ is presumed (Scheme 4, top). Halide abstraction from **1** using $B(C_6F_5)_3$ is rapid (RT, < 5 min) and yields the ionic complex $[(CDP)Bi\cdots ClB(C_6F_5)_3]$ (**10**, Figure 7), which also

reacts rapidly with $PhSiH_3$ to form **9** (Scheme 4). An isolated, metal-free B–Cl/Si–H metathesis (e.g., $[NBu_4][ClB(C_6F_5)_3]$ + excess $PhSiH_3$) required prolonged reaction times and/or heat (see Figure S51), which suggests that bismuth is involved in the formation of **9**. However, this does not necessarily confirm hydride abstraction from the metal because Lewis acids are known to promote adduct formation between silanes and boranes, which are typically in dynamic equilibrium.[67, 68] In this case, no reaction was observed between $B(C_6F_5)_3$ and $PhSiH_3$ at room temperature, but the subsequent addition of **1** may yet result in a simple halide abstraction or anion exchange with the transient silylium-hydridoborate in lieu of hydride abstraction from [Bi]–H.[69]

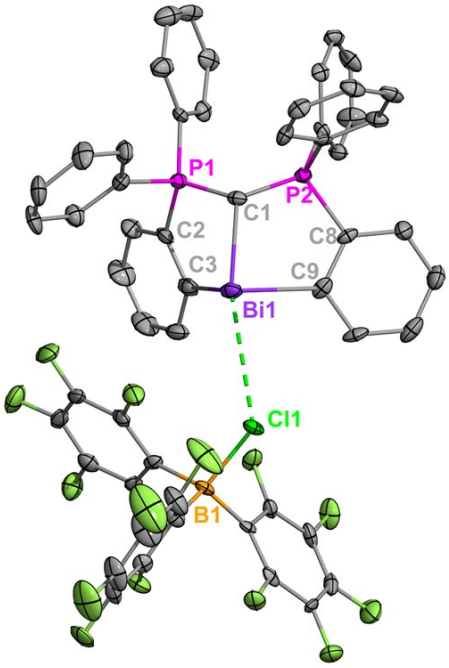

Figure 7. Molecular structure of **10**. Thermal ellipsoids are shown at 50 % probability, and aromatic protons omitted for clarity. Selected bond distances (Å) and angles (°): Bi1–C1,

2.259(5); Bi1–Cl1, 3.4142(18); B1–Cl1, 1.942(6); Bi1–C3, 2.293(6); Bi1–C9, 2.264(6); C1–P1, 1.695(6); C1–P2, 1.686(6); C3–Bi1–C9, 102.7(2); P1–C1–P2, 132.7(4).

Theoretical analysis

To shed light on the bonding situation of the new bismuth complexes, electronic structure calculations for **1**, **2** and **5**$^{+}$ were carried out at the BP86-D3(BJ)/def2-TZVPP level. Considering the crystal-packing effect in experimental structures and the error bar of a given level of theory, the computed geometrical parameters are in good agreement with the experimental values, except for the Bi–X (X = Cl, Br) bond distances in the halido complexes, which are significantly shorter than the corresponding experimental values (Figure S61). The elongated Bi–halide bonds are partially attributed to solvent (DCM) interactions with the halide ligands through H-bonding in the crystal structures. To account for solvent effects, we reoptimized the complexes by employing polarizable continuum model (PCM) and DCM as a solvent. The corresponding structures with geometrical parameters given in Figure S62 show much improved agreement with experimental values, and were thus considered for bonding analysis. Notably, *trans* effect also plays a partial role in the elongation of Bi–X bonds in **1** and **2** since CDP σ-donation populates the Bi–X σ* anti-bonding orbital. Indeed, the experimental Bi–X bond distances are significantly longer than the typical covalent bond distances computed from their covalent radii (Bi–Cl: 2.50 Å, Bi–Br: 2.65 Å)[61] or the parent salts $BiCl_3$ (2.455 Å) and $BiBr_3$ (2.613 Å) calculated at the same level. Complex **9** was also optimized at the BP86-D3(BJ)/def2-SVP level with implicit solvation (PCM, DCM). Compared to the

experimental structure, the calculated Bi1···H1 bond distance is significantly shorter, and the nearly linear Bi1···H1–B1 bond angle in **9** is significantly bent (Figure S62). This disparity is partially rationalized by crystal packing effects. In the crystal structure, the $HB(C_6F_5)_3$ anion is further interacting with an adjacent (CDP)Bi unit through van der Waals' interaction (Figure S63). Because only one (CDP)Bi···$HB(C_6F_5)_3$ unit is considered in our calculations, this intermolecular interaction is missing, and $HB(C_6F_5)_3$ orients sideways to maximize dispersion between C_6F_5 rings in the anion and phenyl rings of CDP. Therefore, to get a more reliable picture of Bi···H bonding nature, we considered the experimental geometry for bonding analysis.

First, we performed a quantum theory of atoms-in-molecules (QTAIM) analysis to gain insight into the topology of the electron density in these complexes.[70] Figure 8 displays the contour plots of Laplacian of electron density ($\nabla^2\rho(r)$) at the ^{CDP}C–Bi–^{Ph}C (H–Bi–^{Ph}C for **9**) plane, where red dotted regions show the electron density accumulated region ($\nabla^2\rho(r) < 0$) and blue solid lines indicate electron density depleted region ($\nabla^2\rho(r) > 0$). The large electron density around both ^{CDP}C and ^{Ph}C is polarized towards the Bi center, although the bond critical point (BCP) is located at $\nabla^2\rho(r) > 0$ region, which is very common for polar covalent bonds and bonds involving heavy elements. This is because $\nabla^2\rho(r_c)$ value is derived from the sum of the three curvature values (λ_1, λ_2 and λ_3), wherein the curvature (λ_3) along the bond axis is always positive and the other two perpendicular to it are negative. Therefore, the criterion of a negative $\nabla^2\rho(r_c)$ value at the BCP for a covalent bond would depend on the condition $\lambda_1 + \lambda_2 > \lambda_3$. However, this is not always the case, especially for bonds involving heavy elements or

polar bonds (including a simple F_2 molecule).[71] The energy density $H(r_c)$, proposed by Kraka and Cremer, is a more effective descriptor in these cases.[71] It is negative at the BCP for covalent bonds and positive for non-covalent bonds. In the present cases, $H(r_c)$ is negative for both ^{CDP}C–Bi and ^{Ph}C–Bi bonds, which indicates covalent character, and the degree of covalency is somewhat larger in the latter bond than in the former. For all the systems, the ^{Ph}C–Bi bonds have similar $H(r_c)$ values, and the covalent character for ^{CDP}C–Bi is larger in **5**$^{+}$ than in **1** and **2**. In complex **9**, there is a maximum electron density path between Bi and H, which is non-covalent in nature as understood from the positive $H(r_c)$ value.

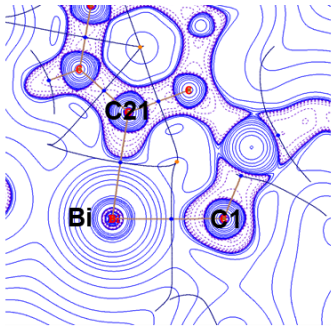

1
^{CDP}**C–Bi:** $\nabla^2\rho(r_c)$ = 0.100 au;
$H(r_c)$ = -0.018 au; $\varepsilon(r_c)$ = 0.03
^{Ph}**C–Bi:** $\nabla^2\rho(r_c)$ = 0.082/0.080 au;
$H(r_c)$ = -0.031/-0.030 au; $\varepsilon(r_c)$ = 0.08/0.08

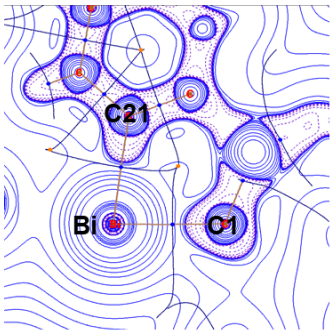

2
^{CDP}**C–Bi:** $\nabla^2\rho(r_c)$ = 0.101 au;
$H(r_c)$ = -0.019 au; $\varepsilon(r_c)$ = 0.03
^{Ph}**C–Bi:** $\nabla^2\rho(r_c)$ = 0.082/0.080 au;
$H(r_c)$ = -0.031/-0.030 au; $\varepsilon(r_c)$ = 0.08/0.08

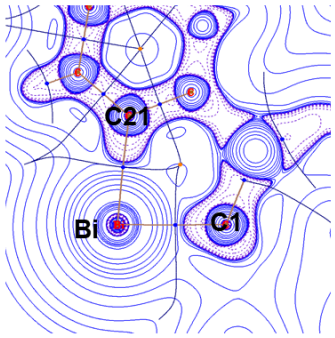

5^{+}
^{CDP}**C–Bi:** $\nabla^2\rho(r_c)$ = 0.104 au;
$H(r_c)$ = -0.030 au; $\varepsilon(r_c)$ = 0.05
^{Ph}**C–Bi:** $\nabla^2\rho(r_c)$ = 0.086/0.083 au;
$H(r_c)$ = -0.033/-0.031 au; $\varepsilon(r_c)$ = 0.06/0.06

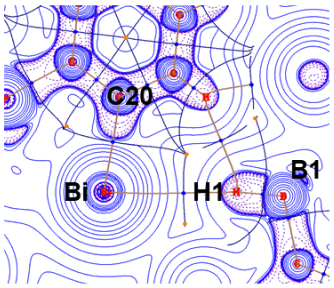

9
^{CDP}**C–Bi:** $\nabla^2\rho(r_c)$ = 0.113 au;
$H(r_c)$ = -0.028 au; $\varepsilon(r_c)$ = 0.04
^{Ph}**C–Bi:** $\nabla^2\rho(r_c)$ = 0.087/0.091 au;
$H(r_c)$ = -0.035/-0.037 au; $\varepsilon(r_c)$ = 0.07/0.07
Bi–H: $\nabla^2\rho(r_c)$ = 0.015 au ; $H(r_c)$ = 0.001 au

Figure 8. The contour plots of Laplacian of electron density at the plane of ^{CDP}C-Bi-^{Ph}C of the studied complexes at the BP86-D3(BJ)/def2-TZVPP level including solvation effect where blue solid lines show $\nabla^2\rho(r) > 0$ and red dotted lines show $\nabla^2\rho(r) < 0$. For complex **9**, experimental geometry is considered.

The ellipticity values ($\varepsilon(r_c)$) at the BCP of ^{CDP}C–Bi and ^{Ph}C–Bi bonds are also given in Figure 8. In single and triple bonds, $\varepsilon(r_c)$ is close to zero because of the cylindrical contour of electron density, whereas in double bonds the asymmetrical electron distribution perpendicular to the bond path results in an elliptical contour of electron density ($\varepsilon(r_c) > 0$). It is well-known that CDP is a strong σ-donor and weak π-donor, and its π-donating ability depends on the correct symmetry and orientation of the acceptor orbital as well as the electrophilicity of that fragment.[72-74] In the present cases, $\varepsilon(r_c)$ values for ^{CDP}C–Bi bonds are nearly zero (0.03 - 0.05) which indicates the absence of any effective double dative bond between ^{CDP}C and Bi. Natural bond orbital (NBO) analyses corroborate these observations, where only one 2c-2e ^{CDP}C–Bi σ-bond is identified, whereas the two π electrons on ^{CDP}C are described as a lone pair (LP) (see Table S6). The Mayer bond orders (MBO) for ^{CDP}C–Bi range from 0.58 (**1**) – 0.81 (**5**$^{+}$), indicating ^{CDP}C→Bi dative bond character. On the other hand, ^{Ph}C–Bi bond orders are very close to the ideal single bond. Minimal ^{CDP}C→Bi π dative interaction is also evident upon inspection of the frontier molecular orbitals (Figure 9). The acceptor orbital of Bi is *sd* hybridized with minor *p*-orbital contribution, but it is not properly oriented

to engage with the π lone pair on CDP. This contrasts with our previously reported CDC-Bi(III) complexes where double dative interactions were noted in their ^{CDC}C–Bi bonds.[47]

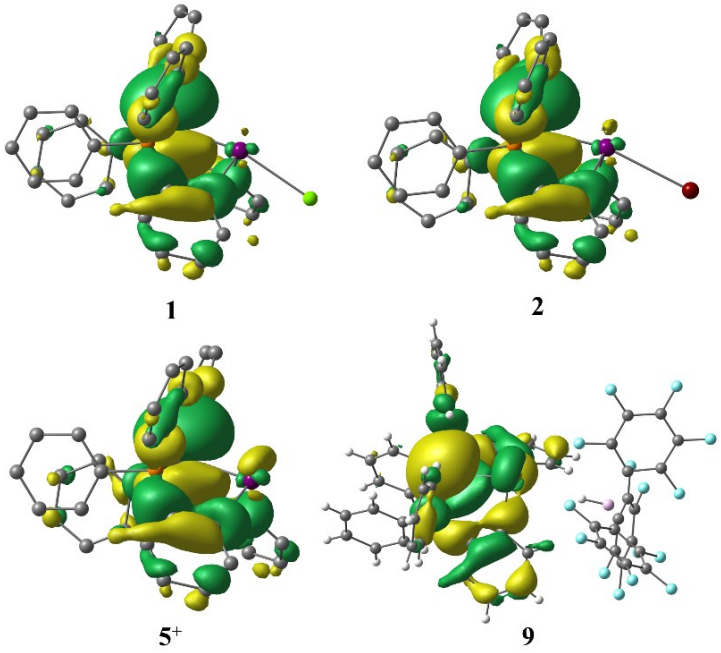

Figure 9. The highest occupied molecular orbital (HOMO) showing π lone-pair on CDP (HOMO-6 for **9**). A low isovalue of 0.02 au is used to visualize the small MO coefficient on Bi center.

CONCLUSION

The dianionic carbodiphosphoranyl ligand framework enabled multi-dimensional bonding and reactivity at bismuth centers featuring a carbon-based donor ligand, as well as redox-flexibility at both metal and ligand. In contrast to known carbone-bismuth complexes which are highly prone to deleterious ligand protonation under air or moisture, compounds **1** and **2** are air stable and the carbone center can be reversibly protonated while retaining metal-

ligand coordination. The latter feature is desirable for developing productive bond activation processes involving proton shuttling or ligand cooperativity. Compounds **1** and **2** also feature carbone *trans* effect, which is unprecedented among the heavy pnictogens, and partially responsible for their remarkable activity for catalytic TEMPO silylation. Such bismuth-mediated thermal dehydrocoupling reactions are typically slow, but we have observed high activities under mild conditions (50 ºC) and low catalyst loadings (5-10 mol%), which compete with or even rival, known Bi(II)/Bi(III) systems. Although the putative intermediates (i.e., $[Bi^{III}]$–H, $[Bi^{III}]$–OTEMP, $[Bi^{II}]^{\cdot}$) are elusive, the reaction of **1**, $PhSiH_3$ and $B(C_6F_5)_3$ yielded the first isolable bismuth hydridoborate (**9**), in a manner that suggests hydride abstraction from a short-lived $[Bi^{III}]$–H species. Quantum chemical bonding analyses of these complexes suggest predominantly $^{carbone}C\rightarrow Bi$ dative bonding through the CDP σ-lone-pair with little involvement of the π-lone-pair. However, the ability to selectively tune the strength of the $^{carbone}C\rightarrow Bi$ interaction by ionization or reversible protonation is desirable for modulating the reactivity of bismuth complexes stabilized by this ligand framework.

ASSOCIATED CONTENT

Supporting Information. The Supporting Information is available free of charge at DOI. Experimental procedures, NMR and IR spectra, crystallographic refinement details (PDF).

Accession Codes

CCDC 2190026-2190029, 2190032-2190046 and 2190048-2190053 contain the supplementary crystallographic data for this paper. These data can be obtained free of charge from The Cambridge Crystallographic Data Centre via www.ccdc.cam.ac.uk/structures

AUTHOR INFORMATION

Corresponding Authors

*E-mail: pans@chemie.uni-marburg.de

*Email: rjg8s@virginia.edu

ORCID

Akachukwu D. Obi: 0000-0001-7118-7931

Diane A. Dickie: 0000-0003-0939-3309

William Tiznado: 0000-0002-6061-8879

Gernot Frenking: 0000-0003-1689-1197

Sudip Pan: 0000-0003-3172-926X

Robert J. Gilliard, Jr.: 0000-0002-8830-1064

Notes

The authors declare no competing financial interest.

ACKNOWLEDGMENT

The authors acknowledge the University of Virginia (UVa), the American Chemical Society Petroleum Research Fund (62280-DNI3), and the National Science Foundation MRI program (CHE-2018870) for support of this work. A.D.O. thanks the Jefferson Scholars Foundation (UVa) for a Burn Family Melville Foundation Graduate Fellowship. S.P. and W.T. thank the financial support of the National Agency for Research and Development (ANID) through FONDECYT projects 1211128. We also thank Hannah Ketcham (University of Virginia) for assistance with GC-MS experiments.

REFERENCES

1. Moon, H. W.; Cornella, J., Bismuth Redox Catalysis: An Emerging Main-Group Platform for Organic Synthesis. *ACS Catal.* **2022,** *12*, 1382-1393.

2. Lipshultz, J. M.; Li, G.; Radosevich, A. T., Main Group Redox Catalysis of Organopnictogens: Vertical Periodic Trends and Emerging Opportunities in Group 15. *J. Am. Chem. Soc.* **2021,** *143*, 1699-1721.

3. Coughlin, O.; Benjamin, S. L., 3.11 - Arsenic, Antimony and Bismuth. In *Comprehensive Coordination Chemistry III*, Constable, E. C.; Parkin, G.; Que Jr, L., Eds. Elsevier: Oxford, 2021, https://doi.org/10.1016/B978-0-08-102688-5.00051-9 pp 321-417.

4. Cornella, J.; Pang, Y., Organometallic Compounds of Arsenic, Antimony and Bismuth. In *Reference Module in Chemistry, Molecular Sciences and Chemical Engineering*, Elsevier: 2021, https://doi.org/10.1016/B978-0-12-820206-7.00128-1.

5. Chitnis, S. S.; Hynes, T., Antimony and Bismuth Complexes in Organic Synthesis. In *Reference Module in Chemistry, Molecular Sciences and Chemical Engineering*, Elsevier: 2021, https://doi.org/10.1016/B978-0-12-820206-7.00025-1.

6. Mohan, R., Green bismuth. *Nat. Chem.* **2010,** *2*, 336-336.

7. Power, P. P., Main-group elements as transition metals. *Nature* **2010,** *463*, 171-177.

8. Weetman, C.; Inoue, S., The Road Travelled: After Main-Group Elements as Transition Metals. *ChemCatChem* **2018,** *10*, 4213-4228.

9. Wedler, H. B.; Wendelboe, P.; Power, P. P., Second-Order Jahn–Teller (SOJT) Structural Distortions in Multiply Bonded Higher Main Group Compounds. *Organometallics* **2018,** *37*, 2929-2936.

10. Power, P. P., An Update on Multiple Bonding between Heavier Main Group Elements: The Importance of Pauli Repulsion, Charge-Shift Character, and London Dispersion Force Effects. *Organometallics* **2020,** *39*, 4127-4138.

11. Abbenseth, J.; Goicoechea, J. M., Recent developments in the chemistry of non-trigonal pnictogen pincer compounds: from bonding to catalysis. *Chem. Sci.* **2020,** *11*, 9728-9740.

12. Lichtenberg, C., Molecular bismuth(iii) monocations: structure, bonding, reactivity, and catalysis. *Chem. Commun.* **2021,** *57*, 4483-4495.

13. Andleeb, S.; Imtiaz ud, D., Recent progress in designing the synthetic strategies for bismuth based complexes. *J. Organomet. Chem.* **2019,** *898*, 120871.

14. Ishida, S.; Hirakawa, F.; Furukawa, K.; Yoza, K.; Iwamoto, T., Persistent Antimony- and Bismuth-Centered Radicals in Solution. *Angew. Chem. Int. Ed.* **2014,** *53*, 11172-11176.

15. Schwamm, R. J.; Lein, M.; Coles, M. P.; Fitchett, C. M., Catalytic oxidative coupling promoted by bismuth TEMPOxide complexes. *Chem. Commun.* **2018,** *54*, 916-919.

16. Ramler, J.; Krummenacher, I.; Lichtenberg, C., Well-Defined, Molecular Bismuth Compounds: Catalysts in Photochemically Induced Radical Dehydrocoupling Reactions. *Chem. Eur. J.* **2020,** *26*, 14551-14555.

17. Mukhopadhyay, D. P.; Schleier, D.; Wirsing, S.; Ramler, J.; Kaiser, D.; Reusch, E.; Hemberger, P.; Preitschopf, T.; Krummenacher, I.; Engels, B.; Fischer, I.; Lichtenberg, C., Methylbismuth: an organometallic bismuthinidene biradical. *Chem. Sci.* **2020,** *11*, 7562-7568.

18. Oberdorf, K.; Hanft, A.; Ramler, J.; Krummenacher, I.; Bickelhaupt, F. M.; Poater, J.; Lichtenberg, C., Bismuth Amides Mediate Facile and Highly Selective Pn–Pn Radical-Coupling Reactions (Pn=N, P, As). *Angew. Chem. Int. Ed.* **2021,** *60*, 6441-6445.

19. Schwamm, R. J.; Lein, M.; Coles, M. P.; Fitchett, C. M., Bi–P Bond Homolysis as a Route to Reduced Bismuth Compounds and Reversible Activation of P4. *Angew. Chem. Int. Ed.* **2016,** *55*, 14798-14801.

20. Planas, O.; Wang, F.; Leutzsch, M.; Cornella, J., Fluorination of arylboronic esters enabled by bismuth redox catalysis. *Science* **2020,** *367*, 313-317.

21. Ramler, J.; Krummenacher, I.; Lichtenberg, C., Bismuth Compounds in Radical Catalysis: Transition Metal Bismuthanes Facilitate Thermally Induced Cycloisomerizations. *Angew. Chem. Int. Ed.* **2019,** *58*, 12924-12929.

22. Pang, Y.; Leutzsch, M.; Nöthling, N.; Cornella, J., Catalytic Activation of N2O at a Low-Valent Bismuth Redox Platform. *J. Am. Chem. Soc.* **2020,** *142*, 19473-19479.

23. Gimferrer, M.; Danés, S.; Andrada, D. M.; Salvador, P., Unveiling the Electronic Structure of the Bi(+1)/Bi(+3) Redox Couple on NCN and NNN Pincer Complexes. *Inorg. Chem.* **2021,** *60*, 17657-17668.

24. Schwamm, R. J.; Harmer, J. R.; Lein, M.; Fitchett, C. M.; Granville, S.; Coles, M. P., Isolation and Characterization of a Bismuth(II) Radical. *Angew. Chem. Int. Ed.* **2015,** *54*, 10630-10633.

25. Turner, Z. R., Bismuth Pyridine Dipyrrolide Complexes: a Transient Bi(II) Species Which Ring Opens Cyclic Ethers. *Inorg. Chem.* **2019,** *58*, 14212-14227.

26. Ramler, J.; Schwarzmann, J.; Stoy, A.; Lichtenberg, C., Two Faces of the Bi–O Bond: Photochemically and Thermally Induced Dehydrocoupling for Si–O Bond Formation. *Eur. J. Inorg. Chem.* **2022,** *2022*, e202100934.

27. Kindervater, M. B.; Marczenko, K. M.; Werner-Zwanziger, U.; Chitnis, S. S., A Redox-Confused Bismuth(I/III) Triamide with a T-Shaped Planar Ground State. *Angew. Chem. Int. Ed.* **2019,** *58*, 7850-7855.

28. Deb, R.; Balakrishna, P.; Majumdar, M., Recent Developments in the Chemistry of Pn(I) (Pn=N, P, As, Sb, Bi) Cations. *Chem. Asian J.* **2022,** *17*, e202101133.

29. Wang, F.; Planas, O.; Cornella, J., Bi(I)-Catalyzed Transfer-Hydrogenation with Ammonia-Borane. *J. Am. Chem. Soc.* **2019,** *141*, 4235-4240.

30. Šimon, P.; de Proft, F.; Jambor, R.; Růžička, A.; Dostál, L., Monomeric Organoantimony(I) and Organobismuth(I) Compounds Stabilized by an NCN Chelating Ligand: Syntheses and Structures. *Angew. Chem. Int. Ed.* **2010,** *49*, 5468-5471.

31. Nesterov, V.; Reiter, D.; Bag, P.; Frisch, P.; Holzner, R.; Porzelt, A.; Inoue, S., NHCs in Main Group Chemistry. *Chem. Rev.* **2018,** *118*, 9678-9842.

32. Deka, R.; Orthaber, A., Carbene chemistry of arsenic, antimony, and bismuth: origin, evolution and future prospects. *Dalton Trans.* **2022,** *51*, 8540-8556.

33. Aprile, A.; Corbo, R.; Vin Tan, K.; Wilson, D. J. D.; Dutton, J. L., The first bismuth–NHC complexes. *Dalton Trans.* **2014,** *43*, 764-768.

34. Wang, G.; Freeman, L. A.; Dickie, D. A.; Mokrai, R.; Benkő, Z.; Gilliard, R. J., Highly Reactive Cyclic(alkyl)(amino) Carbene- and N-Heterocyclic Carbene-Bismuth(III) Complexes: Synthesis, Structure, and Computations. *Inorg. Chem.* **2018,** *57*, 11687-11695.

35. Waters, J. B.; Chen, Q.; Everitt, T. A.; Goicoechea, J. M., N-Heterocyclic carbene adducts of the heavier group 15 tribromides. Normal to abnormal isomerism and bromide ion abstraction. *Dalton Trans.* **2017,** *46*, 12053-12066.

36. Wilson, D. J. D.; Couchman, S. A.; Dutton, J. L., Are N-Heterocyclic Carbenes "Better" Ligands than Phosphines in Main Group Chemistry? A Theoretical Case Study of Ligand-Stabilized E2 Molecules, L-E-E-L (L = NHC, phosphine; E = C, Si, Ge, Sn, Pb, N, P, As, Sb, Bi). *Inorg. Chem.* **2012,** *51*, 7657-7668.

37. Walley, J. E.; Warring, L. S.; Kertész, E.; Wang, G.; Dickie, D. A.; Benkő, Z.; Gilliard, R. J., Indirect Access to Carbene Adducts of Bismuth- and Antimony-Substituted Phosphaketene and Their Unusual Thermal Transformation to Dipnictines and [(NHC)2OCP][OCP]. *Inorg. Chem.* **2021,** *60*, 4733-4743.

38. Wang, G.; Freeman, L. A.; Dickie, D. A.; Mokrai, R.; Benkő, Z.; Gilliard, R. J., Isolation of Cyclic(Alkyl)(Amino) Carbene–Bismuthinidene Mediated by a Beryllium(0) Complex. *Chem. Eur. J.* **2019,** *25*, 4335-4339.

39. Siddiqui, M. M.; Sarkar, S. K.; Nazish, M.; Morganti, M.; Köhler, C.; Cai, J.; Zhao, L.; Herbst-Irmer, R.; Stalke, D.; Frenking, G.; Roesky, H. W., Donor-Stabilized Antimony(I) and Bismuth(I) Ions: Heavier Valence Isoelectronic Analogues of Carbones. *J. Am. Chem. Soc.* **2021,** *143*, 1301-1306.

40. Tonner, R.; Öxler, F.; Neumüller, B.; Petz, W.; Frenking, G., Carbodiphosphoranes: The Chemistry of Divalent Carbon(0). *Angew. Chem. Int. Ed.* **2006,** *45*, 8038-8042.

41. Ramirez, F.; Desai, N. B.; Hansen, B.; McKelvie, N., HEXAPHENYLCARBODIPHOSPHORANE, (C6H5)3PCP(C6H5)3. *J. Am. Chem. Soc.* **1961,** *83*, 3539-3540.

42. Dobrovetsky, R.; Stephan, D. W., Catalytic Reduction of CO2 to CO by Using Zinc(II) and In Situ Generated Carbodiphosphoranes. *Angew. Chem. Int. Ed.* **2013,** *52*, 2516-2519.

43. Dyker, C. A.; Lavallo, V.; Donnadieu, B.; Bertrand, G., Synthesis of an extremely bent acyclic allene (a "carbodicarbene"): a strong donor ligand. *Angew. Chem. Int. Ed.* **2008,** *47*, 3206-9.

44. Tonner, R.; Frenking, G., C(NHC)2: Divalent Carbon(0) Compounds with N-Heterocyclic Carbene Ligands—Theoretical Evidence for a Class of Molecules with Promising Chemical Properties. *Angew. Chem. Int. Ed.* **2007,** *46*, 8695-8698.

45. Chen, W.-C.; Hsu, Y.-C.; Lee, C.-Y.; Yap, G. P. A.; Ong, T.-G., Synthetic Modification of Acyclic Bent Allenes (Carbodicarbenes) and Further Studies on Their Structural Implications and Reactivities. *Organometallics* **2013,** *32*, 2435-2442.

46. Liu, S.-k.; Shih, W.-C.; Chen, W.-C.; Ong, T.-G., Carbodicarbenes and their Captodative Behavior in Catalysis. *ChemCatChem* **2018,** *10*, 1483-1498.

47. Walley, J.; Warring, L.; Wang, G.; Dickie, D. A.; Pan, S.; Frenking, G.; Gilliard, R. J., Carbodicarbene Bismaalkene Cations: Unravelling the Complexities of Carbene versus Carbone in Heavy Pnictogen Chemistry. *Angew. Chem. Int. Ed.* **2021,** *60*, 6682-6690.

48. Thirumoorthi, R.; Chivers, T.; Gendy, C.; Vargas-Baca, I., CH–NH Tautomerism in the Products of the Reactions of the Methanide [HC(PPh2NSiMe3)2]– with Pnictogen and Tellurium Iodides. *Organometallics* **2013,** *32*, 5360-5373.

49. Thirumoorthi, R.; Chivers, T.; Vargas-Baca, I., S,C,S-Pnictogen bonding in pincer complexes of the methanediide [C(Ph2PS)2]2–. *Dalton Trans.* **2011,** *40*, 8086-8088.

50. Sindlinger, C. P.; Stasch, A.; Wesemann, L., Heavy Group 15 Element Compounds of a Sterically Demanding Bis(iminophosphorane)methanide and -methanediide. *Organometallics* **2014,** *33*, 322-328.

51. Münzer, J. E.; Kneusels, N.-J. H.; Weinert, B.; Neumüller, B.; Kuzu, I., Hexaphenyl carbodiphosphorane adducts of heavier group 15 element trichlorides: syntheses, properties and reactivities. *Dalton Trans.* **2019,** *48*, 11076-11085.

52. Böttger, S. C.; Poggel, C.; Sundermeyer, J., ortho-Directed Dilithiation of Hexaphenyl-carbodiphosphorane. *Organometallics* **2020,** *39*, 3789-3793.

53. Buchner, M. R.; Pan, S.; Poggel, C.; Spang, N.; Müller, M.; Frenking, G.; Sundermeyer, J., Di-ortho-beryllated Carbodiphosphorane: A Compound with a Metal–Carbon Double Bond to an Element of the s-Block. *Organometallics* **2020,** *39*, 3224-3231.

54. Henceforth, the carbodiphosphoranyl dianion is denoted as "CDP" whereas the neutral carbodiphosphorane ligand will be specifically described as "neutral CDP" or "monodentate CDP"

55. Notably, several solvates of **1** and **2**, as well as most of the compounds described in this manuscript, were crystallographically identified, and their cifs included in the supporting information

56. Balasubramaniam, S.; Kumar, S.; Andrews, A. P.; Varghese, B.; Jemmis, E. D.; Venugopal, A., A Dicationic Bismuth(III) Lewis Acid: Catalytic Hydrosilylation of Olefins. *Eur. J. Inorg. Chem.* **2019,** *2019*, 3257-3257.

57. Bao, M.; Hayashi, T.; Shimada, S., Cationic Organobismuth Complex with 5,6,7,12-Tetrahydrodibenz[c,f][1,5]azabismocine Framework and Its Coordination Complexes with Neutral Molecules. *Organometallics* **2007,** *26*, 1816-1822.

58. Toma, A.; Raț, C. I.; Silvestru, A.; Rüffer, T.; Lang, H.; Mehring, M., Heterocyclic bismuth(III) compounds with transannular S→Bi interactions. An experimental and theoretical approach. *J. Organomet. Chem.* **2016,** *806*, 5-11.

59. Yin, S.-F.; Maruyama, J.; Yamashita, T.; Shimada, S., Efficient Fixation of Carbon Dioxide by Hypervalent Organobismuth Oxide, Hydroxide, and Alkoxide. *Angew. Chem. Int. Ed.* **2008,** *47*, 6590-6593.

60. Shimada, S.; Yamazaki, O.; Tanaka, T.; Suzuki, Y.; Tanaka, M., Synthesis and structure of 5,6,7,12-tetrahydrodibenz[c,f][1,5]azabismocines. *J. Organomet. Chem.* **2004,** *689*, 3012-3023.

61. Pyykkö, P.; Atsumi, M., Molecular Single-Bond Covalent Radii for Elements 1–118. *Chem. Eur. J.* **2009,** *15*, 186-197.

62. Casely, I. J.; Ziller, J. W.; Mincher, B. J.; Evans, W. J., Bismuth Coordination Chemistry with Allyl, Alkoxide, Aryloxide, and Tetraphenylborate Ligands and the {[2,6-(Me2NCH2)2C6H3]2Bi}+ Cation. *Inorg. Chem.* **2011,** *50*, 1513-1520.

63. Jones, C., Dimeric magnesium(I) β-diketiminates: a new class of quasi-universal reducing agent. *Nat. Rev. Chem.* **2017,** *1*, 0059.

64. Carden, J. L.; Dasgupta, A.; Melen, R. L., Halogenated triarylboranes: synthesis, properties and applications in catalysis. *Chem. Soc. Rev.* **2020,** *49*, 1706-1725.

65. Roy, M. M. D.; Omaña, A. A.; Wilson, A. S. S.; Hill, M. S.; Aldridge, S.; Rivard, E., Molecular Main Group Metal Hydrides. *Chem. Rev.* **2021,** *121*, 12784-12965.

66. Hardman, N. J.; Twamley, B.; Power, P. P., (2,6-Mes2H3C6)2BiH, a Stable, Molecular Hydride of a Main Group Element of the Sixth Period, and Its Conversion to the Dibismuthene (2,6-Mes2H3C6)BiBi(2,6-Mes2C6H3). *Angew. Chem. Int. Ed.* **2000,** *39*, 2771-2773.

67. Houghton, A. Y.; Hurmalainen, J.; Mansikkamäki, A.; Piers, W. E.; Tuononen, H. M., Direct observation of a borane–silane complex involved in frustrated Lewis-pair-mediated hydrosilylations. *Nat. Chem.* **2014,** *6*, 983-988.

68. Lawson, J. R.; Melen, R. L., Tris(pentafluorophenyl)borane and Beyond: Modern Advances in Borylation Chemistry. *Inorg. Chem.* **2017,** *56*, 8627-8643.

69. Lampland, N. L.; Pindwal, A.; Neal, S. R.; Schlauderaff, S.; Ellern, A.; Sadow, A. D., Magnesium-catalyzed hydrosilylation of α,β-unsaturated esters. *Chem. Sci.* **2015,** *6*, 6901-6907.

70. Bader, R. F. W., *Atoms in Molecules: A Quantum Theory*. Clarendon Press: Oxford, UK, 1990.

71. Cremer, D.; Kraka, E., Chemical Bonds without Bonding Electron Density? Does the Difference Electron-Density Analysis Suffice for a Description of the Chemical Bond? *Angew. Chem. Int. Ed.* **1984,** *23*, 627-628.

72. Frenking, G.; Tonner, R.; Klein, S.; Takagi, N.; Shimizu, T.; Krapp, A.; Pandey, K. K.; Parameswaran, P., New bonding modes of carbon and heavier group 14 atoms Si–Pb. *Chem. Soc. Rev.* **2014,** *43*, 5106-5139.

73. Zhao, L.; Chai, C.; Petz, W.; Frenking, G., Carbones and Carbon Atom as Ligands in Transition Metal Complexes. *Molecules* **2020,** *25*, 4943-4990.

74. Kroll, A.; Steinert, H.; Scharf, L. T.; Scherpf, T.; Mallick, B.; Gessner, V. H., A diamino-substituted carbodiphosphorane as strong C-donor and weak N-donor: isolation of monomeric trigonal-planar L·ZnCl2. *Chem. Commun.* **2020,** *56*, 8051-8054.

For Table of Contents Only

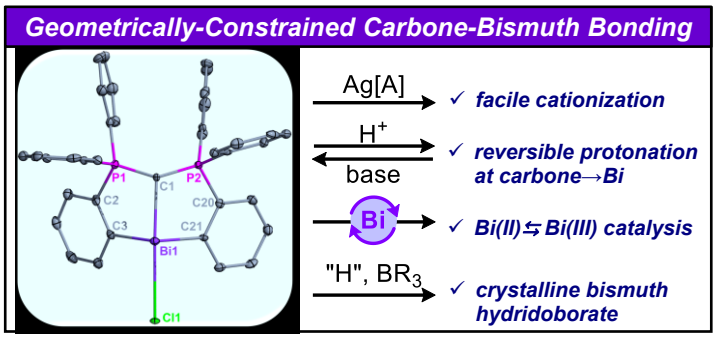

Carbodiphosphorane (CDP) bismuth complexes wherein the bismuth-carbone interactions are geometrically-constrained with pendant phenyl groups have been isolated and characterized. Their bismuth-carbone bonds are highly tunable, and resistant to deleterious hydrolysis. Unprecedented carbone *trans* effect in the halides enables their high catalytic activity for TEMPO silylation, and the putative Bi-H intermediate was captured with $B(C_6F_5)_3$ as the first isolable bismuth hydridoborate.